

Explanation of Normal-State Properties of High-Temperature Superconductors

S. A. Trugman

Theoretical Division, Los Alamos National Laboratory, Los Alamos, New Mexico 87545

(Received 26 April 1990)

The magnetic susceptibility, Hall effect, thermopower, specific heat, and plasma frequency are calculated as a function of doping and temperature for $\text{La}_{2-x}\text{Sr}_x\text{CuO}_4$ and related compounds. There is good quantitative agreement with experiment. The calculation is based on quasiparticles in a Mott insulator, whose dispersion $\epsilon(\mathbf{k})$ is calculated variationally in the t - t' - J model (and the t - J model). The quasiparticles are assumed to form a weakly interacting Fermi liquid, which is treated in the relaxation-time approximation.

PACS numbers: 74.65.+n, 72.15.-v, 75.10.Jm, 75.10.Lp

High-temperature superconductors have unusual normal-state properties that may be the most important clue to their physics. In particular, there have been suggestions that these properties may be incompatible with a Fermi-liquid description.¹ It is shown below that a calculation based on a weakly interacting Fermi liquid (a Fermi gas) of quasiparticles gives good quantitative agreement with several of the measured normal-state properties as a function of both doping and temperature, including magnetic susceptibility, Hall effect, thermopower, specific heat, and plasma frequency. (The resistivity is not calculated for reasons explained near the end.) The quasiparticles are those of the t - t' - J model, which is derived from the one-band Hubbard model in the large- U limit. The quasiparticles that form when a hole is added to the antiferromagnetic Mott insulator with one electron per site are quite different from free electrons by virtue of the cloud of spin flips that they carry with them. The hypothesis being investigated is that most of the normal-state properties can be explained by the dressing of the quasiparticles with spin flips and the subsequent modification of their dispersion relation $\epsilon(\mathbf{k})$. The simplest possible assumptions are made about all other aspects of the problem. The quasiparticles are assumed to fill the rigid band described by the single-hole $\epsilon(\mathbf{k})$, forming a weakly interacting Fermi gas. A very different Fermi-liquid theory is discussed in Refs. 2 and 3. Nagaosa and Lee have recently calculated normal-state properties of the uniform resonating-valence-bond state.⁴

The Hubbard model describes electrons in a tight-binding model with an on-site repulsion U . The t - t' - J model derived from it operates on the subspace with no doubly occupied sites. It has an antiferromagnetic interaction J between neighboring spins, and allows holes to hop to nearest-neighbor sites with amplitude t and to next-nearest-neighbor sites with amplitude $t' = J = t^2/U$.⁵ The quasiparticle $\epsilon(\mathbf{k})$ is obtained for an infinite system by assuming a variational space in which the hole can have several nearby spin flips with respect to the Néel state. The t - t' - J Hamiltonian is then solved exactly in the variational space.⁶ This paper uses 197 variational spin states per lattice site. Work on the t - t' - J model and

on the simplified t - J model is reviewed by Lee.⁷ The predictions below are made primarily for $\text{La}_{2-x}\text{Sr}_x\text{CuO}_4$, but apply to the other high-temperature superconducting compounds provided that the relevant physics occurs in the CuO_2 planes and that the hole density in the CuO_2 planes is known as a function of composition.⁸ It is assumed that $\text{La}_{2-x}\text{Sr}_x\text{CuO}_4$ measurements are not dominated by inhomogeneity, although this is controversial.⁹

Once the quasiparticle band $\epsilon(\mathbf{k})$ has been obtained, the transport and susceptibility are obtained by the standard integrals over the Brillouin zone. Following Ref. 10, the electrical current j in the presence of external \mathbf{E} and \mathbf{B} fields and a thermal gradient ∇T is

$$j_\alpha = \sigma_{\alpha\beta} E_\beta + \sigma_{\alpha\beta\gamma} E_\beta B_\gamma + v_{\alpha\beta} \nabla_\beta T + \dots \quad (1)$$

The transport coefficients in the relaxation-time approximation are

$$\sigma_{\alpha\beta} = \frac{2e^2\tau}{V} \sum_{\mathbf{k}} v_\alpha(\mathbf{k}) v_\beta(\mathbf{k}) \left[-\frac{\partial f}{\partial \epsilon(\mathbf{k})} \right], \quad (2)$$

$$\sigma_{\alpha\beta\gamma} = -\frac{2e^3\tau^2}{\hbar cV} \sum_{\mathbf{k}} v_\alpha(\mathbf{k}) \epsilon_{\lambda\mu\gamma} v_\lambda(\mathbf{k}) \frac{\partial v_\beta(\mathbf{k})}{\partial k_\mu} \left[-\frac{\partial f}{\partial \epsilon(\mathbf{k})} \right], \quad (3)$$

$$v_{\alpha\beta} = \frac{2e\tau}{VT} \sum_{\mathbf{k}} v_\alpha(\mathbf{k}) v_\beta(\mathbf{k}) [\epsilon(\mathbf{k}) - \mu] \left[-\frac{\partial f}{\partial \epsilon(\mathbf{k})} \right], \quad (4)$$

where the factors of 2 account for up and down quasiparticle spins, V is the volume, $\epsilon_{\lambda\mu\gamma}$ is the completely antisymmetric tensor, and $\hbar v_\alpha = \partial \epsilon / \partial k_\alpha$. The relaxation time τ can be dominated by interactions between a quasiparticle and impurities, phonons, spin fluctuations, or other quasiparticles. The \mathbf{k} sums are over the antiferromagnetic Brillouin zone. The Fermi function is $f = \{\exp[(\epsilon - \mu)/k_B T] + 1\}^{-1}$. The sums are done numerically using a 40×80 grid for the antiferromagnetic zone. Because the variational calculation is for an infinite system, $\epsilon(\mathbf{k})$ can be obtained for arbitrary \mathbf{k} . It can thus describe processes dominated by arbitrarily low-energy particle-hole excitations, which a small-lattice calculation cannot. (It may be possible to use

small-system results by varying boundary conditions.)

The Hall resistivity is $R_{xy}^H \equiv E_y/j_x B_z = \sigma_{xyz}/\sigma_{xx}\sigma_{yy}$. In this approximation, R^H is independent of the scattering time τ . The thermoelectric tensor $S_{\alpha\beta}$ gives the induced electric field when no current flows,

$$E_\alpha = S_{\alpha\beta} \nabla_\beta T = -(\sigma^{-1})_{\alpha\gamma} v_{\gamma\beta} \nabla_\beta T. \quad (5)$$

The tensors σ , v , and S are diagonal for this problem. Finally, the Pauli magnetic susceptibility χ is given by

$$\chi = (g_0 \mu_B^2 / V) \sum_{\mathbf{k}} [-\partial f / \partial \epsilon(\mathbf{k})], \quad (6)$$

where μ_B is the Bohr magneton. As the quasiparticle dresses itself with spin flips, the spin component S_z is conserved, so that $g_0 = 2$, the bare electron g factor.

The t - t' - J model has one dimensionless parameter, U/t , the ratio of the on-site repulsion to the hopping amplitude. The data warrant only a rough fitting of parameters, taken to be $U/t = 12$ and $t = 1.6$ eV to fit the susceptibility data (see below). These parameters are used throughout this paper. The fit to experiment would not be drastically worse if the values for U and t were taken from other calculations.¹¹

The Fermi surface in the repeated-zone scheme is shown in Fig. 1. Significant temperature dependence arises from the $-\partial f / \partial \epsilon$ term because the quasiparticle band is quite flat; $\epsilon(\pi, 0) - \epsilon(\pi/2, \pi/2)$ is only 0.10 eV. Because of the long-range antiferromagnetic order of the Mott insulating state, the quasiparticle energy $\epsilon(\mathbf{k})$ is periodic outside of the reduced zone. True long-range

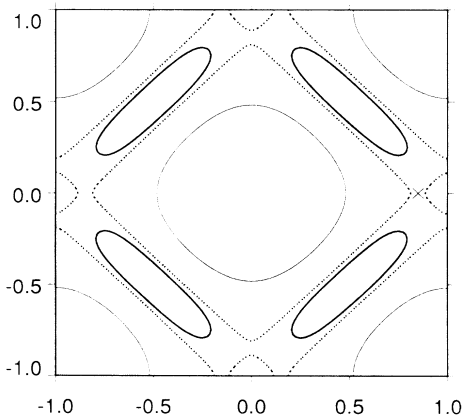


FIG. 1. As x is varied, the Fermi surface has three distinct topologies, which change at $x_1 = 0.262$ and at $x_2 = 0.311$. For $0 < x < x_1$, the Fermi surface consists of eccentric ellipses, shown as heavy lines for $x = 0.116$. The interior of an ellipse is filled with quasiholes (or the exterior with quasidelectrons). As x increases, the ellipses grow, until they meet at saddle points (one of which is indicated by a \times) at $x = x_1$. For $x_1 < x < x_2$, the Fermi surface consists of two distinct types of curves, shown as dotted lines for $x = 0.277$. As x approaches x_2 , the smaller piece disappears at the local maximum at $\mathbf{k} = (\pi, 0)$. Finally, for $x_2 < x < 1$, the Fermi surface is an ordinary closed curve centered on the origin, shown as a thin line for $x = 0.664$.

antiferromagnetic order disappears at rather low doping x . Thus, the use of rigid bands implicitly makes the reasonable assumption that the effective energy dispersion $\epsilon(\mathbf{k})$ is sensitive mainly to short-range antiferromagnetic correlations, and not to long-range order.

The theoretical magnetic susceptibility χ as a function of x and temperature is shown in Fig. 2, along with data from Refs. 12 and 13. It is assumed that the measured χ is dominated by the spin susceptibility.¹⁴ The theoretical susceptibility is maximum at $x_1 = 0.26$, where the saddle-point Van Hove singularity in the quasiparticle $\epsilon(\mathbf{k})$ has a logarithmically divergent density of states. The divergence is smoothed at higher temperatures. Below $x \approx 0.17$, the temperature dependence reverses, and χ increases with increasing T at the lowest temperatures. The zero-temperature χ is proportional to the quasiparticle density of states. These features are in good agreement with experiment, including the absolute magnitude of χ . The theory is less accurate at small x . If effects of disorder were added to the theory, the large jump discontinuity in the density of states at the bottom of the quasiparticle band would be smoothed, and agreement with Ref. 12 improved.

The susceptibility changes somewhat as U/t varies. For $U/t = 8, 12$, and 16 , the position of the susceptibility maximum at 50 K assumes the values $x = 0.19, 0.26$, and 0.29 . $U/t = 12$ is chosen to put the position of the maximum near the value observed in Ref. 12. The parameter t is set to 1.6 eV to get the best magnitude and temperature agreement for χ . Once U and t are fixed from the susceptibility data, there are no free parameters for the calculations below on Hall effect, thermopower, specific heat, or plasma frequency.

Figure 3 shows the theoretical Hall resistivity, togeth-

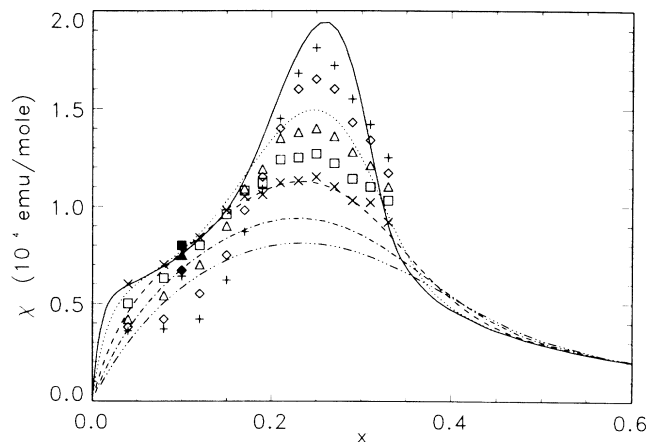


FIG. 2. The magnetic susceptibility χ as a function of doping x at temperatures of 50, 100, 200, 300, and 400 K, shown, respectively, as solid, dotted, dashed, dot-dashed, and triple-dot-dashed lines. The experimental susceptibility at the same temperatures is shown, respectively, by pluses, diamonds, triangles, squares, and crosses (Ref. 12). Solid symbols are single-crystal data (Ref. 13).

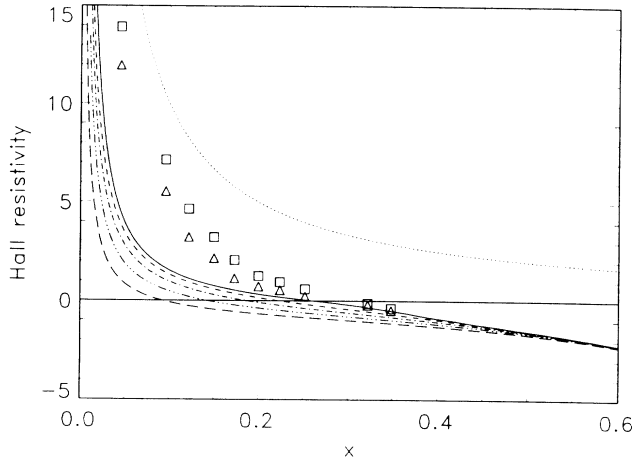


FIG. 3. The Hall resistivity R_H as a function of x at temperatures of 50, 200, 300, 400, and 500 K, shown, respectively, as solid, dashed, dot-dashed, triple-dot-dashed, and long-dashed lines. The experimental R_H is plotted at 80 K (squares) and 300 K (triangles) (Ref. 15). R_H is in units of V_0/ec , where $V_0 = 94.2 \text{ \AA}^3$ is the volume of a formula unit. The upper dotted line plots $R_H = +1/nec$.

er with the data of Takagi *et al.*¹⁵ The experiments are in the low-field regime.¹⁶ The low-temperature theoretical R_H diverges for small x as a positive constant b times $1/nec$, where the hole density n is taken equal to x/V_0 , and V_0 is the volume of a formula unit. R_H changes sign at $x = x_1 = 0.262$. It decreases with increasing temperature, and the temperature dependence is smaller at larger x . All of these features are consistent with the measurements of Ref. 15, including the sign change at a very similar value. The experimental temperature dependence is weaker than that predicted by theory at small x .¹⁶ As proposed above in the context of the susceptibility measurements, this may be due to disorder, which reduces the density of states at small x and thus the temperature dependence. Other Fermi-liquid calculations obtain a Hall resistivity that goes to a constant as $x \rightarrow 0$.^{3,17} Kim, Levin, and Auerbach² obtain a divergence by adding interplanar coupling, but this approach has been criticized by Ong.¹⁶

The Fermi surface of Fig. 1 results in $b < 1$. At small x , the Fermi surface consists of elliptical pockets at right angles to each other. It is straightforward to show that the low-field Hall resistivity is then b/nec , with $b = 4m_1m_2/(m_1+m_2)^2$, where m_1 and m_2 are the effective masses for the ellipses. This gives $b \approx \frac{1}{4}$ for $U/t = 12$. The b of Ref. 15 is larger, approximately $\frac{2}{3}$, and that of Ref. 18 is essentially 1. An experimental b smaller than 1 is also found for the 1:2:3 compounds and for Bi 2:2:1:2.¹⁶ The smaller theoretical b may imply that the theoretical ellipses are too eccentric. At very high temperatures (over 700 K), the theoretical R_H diverges like $1/x$ times a *negative* constant as $x \rightarrow 0$. This occurs when quasiparticles are thermally excited into the electronlike parts of the zone.

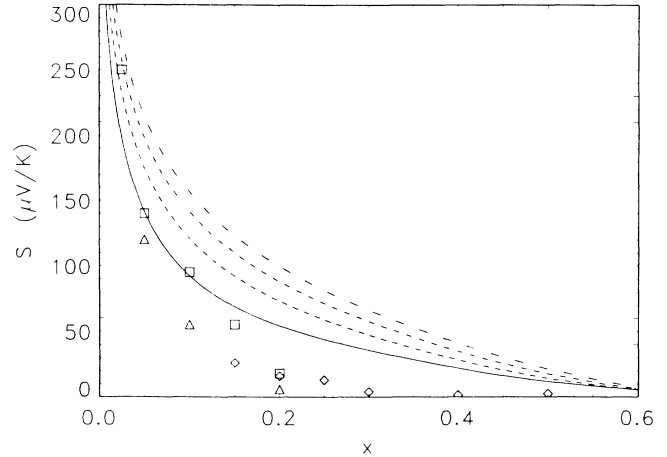


FIG. 4. The thermopower S plotted as a function of x at temperatures of 200, 300, 400, and 500 K, shown, respectively, as solid, dashed, dot-dashed, and triple-dot-dashed lines. The experimental S at room temperature is plotted as squares (Ba doping) and triangles (Sr doping) (Ref. 20). Diamonds denote Sr doping at 240 K (Ref. 19).

The thermopower S obtained from Eq. (5) is shown in Fig. 4. The relaxation time τ is for simplicity assumed energy independent, even though this may not be a satisfactory approximation for some materials. S is independent of τ for constant τ . The theoretical S vanishes at zero temperature and diverges as $x \rightarrow 0$. Although the sign of S nominally measures the sign of the charge carriers, it remains positive (holelike) up to $x \approx 0.7$. This is to be contrasted with the Hall coefficient, which changes sign at $x = 0.26$. S does not change sign when the topology of the Fermi surface changes because it is a complicated integral over the entire Brillouin zone. These properties agree with experiment,^{19,20} including the lack of sign change and large magnitude of S at small x . The experimental S is less temperature dependent than the theory.

The linear term γ in the low-temperature specific heat is given by $\gamma = (2\pi^2 k_B^2/3V) \sum_{\mathbf{k}} \delta[\epsilon(\mathbf{k}) - \mu]$. The theoretical value at $x = 0.1$ is 5.5 mJ/mole K^2 . This is in good agreement with a measurement on a nonsuperconducting single crystal at $x = 0.1$ of $5.1 \pm 0.3 \text{ mJ/mole K}^2$.¹³ A sample from the same batch had a low-temperature c -axis susceptibility of $\chi = 0.64 \times 10^{-4} \text{ emu/mole}$.¹³ The Wilson ratio is defined as $R = (\chi/\gamma) \pi^2 k_B^2/3g^2 \mu_B^2$, which must be 1 at low temperatures for calculations based on noninteracting Fermi quasiparticles, including the present one. The experimental ratio from Ref. 13 is $R = 0.92$, which is consistent with 1 given the uncertainty in χ . Based on other data, Johnston²¹ also finds an experimental $R = 1$. Defining an effective mass m_γ from the theoretical specific heat by assuming two-dimensional parabolic bands, the ratio to the free electron mass is $m_\gamma/m_0 = 3.9$ at $x = 0.1$.

The Drude plasma frequency is calculated from Eq.

(2) using $\Omega_{\rho aa}^2 = (4\pi/\tau)\sigma_{aa}$.¹⁰ The theoretical plasma frequency is only weakly temperature dependent. At 200 K and $x = 0.02, 0.05, 0.1, 0.2, 0.3, 0.4,$ and 0.5 , the respective plasma frequencies $\hbar\Omega_p$ in eV are 0.63, 0.98, 1.31, 1.66, 1.87, 2.07, and 2.28. The extraction of plasma frequencies from infrared reflectivity measurements is controversial.²² Measurements by Tajima *et al.*²³ on single crystals of $\text{La}_{2-x}\text{Sr}_x\text{CuO}_4$ allow the plasma frequency to be determined from the conductivity sum rule, $\Omega_p^2 = 8\int_0^{\omega_c}\sigma(\omega)d\omega$, where ω_c is a cutoff frequency. Their conductivity integral up to 1.5 eV gives plasma frequencies for $x = 0.02, 0.06, 0.1,$ and 0.2 , respectively, of 1.15, 1.43, 1.67, and 1.79 eV. Their attempt to integrate only the Drude part gives, respectively, 0.38, 0.47, 0.54, and 1.21 eV. The present theoretical plasma frequency has the correct x dependence, but is somewhat larger than the experimental Drude plasma frequency. The magnitude is in better agreement than that of local-density-functional calculations, which give $\hbar\Omega_p \approx 3.0$ eV and slowly decreasing with increasing x .¹⁷

Conspicuously absent from the above list of properties is the conductivity $\sigma_{\alpha\beta}$. We cannot calculate τ from first principles, which dominates its temperature dependence. The conductivity integral [Eq. (2)] with the factor of τ removed is proportional to Ω_p^2 given above.

The susceptibility and Hall resistivity were calculated for the t - J model (omitting the t' term) at the same parameters. The curves are qualitatively similar, but differ by about 40% both in magnitude and in the x at which R_H vanishes.

The elliptical hole pockets continuously evolve into a standard circular Fermi surface at high doping, with no phase transition between a Mott-like and Luttinger-like Fermi liquid (except for the topology changes). The calculated Fermi surface has the correct Luttinger volume with respect to the small (antiferromagnetic) Brillouin zone at all doping x . It has the Luttinger volume with respect to the large zone only once the saddle is flooded with holes ($x > x_1 = 0.26$). Other theories that generate a similar quasiparticle $\epsilon(\mathbf{k})$ should give similar results for the calculated properties.^{7,18,24} Finally, it should be noted that superconductivity by almost any mechanism is enhanced by a large density of states. The calculated quasiparticle density of states is nonmonotonic, peaking at about $x_1 = 0.26$, in qualitative agreement with the variation of T_c with doping in the 2:1:4 compounds.

I would like to thank E. Abrahams, R. Albers, P. Allen, N. Ashcroft, B. Brandow, S. Doniach, Z. Fisk, P. Lomdahl, A. Migliori, P. Monthoux, N. P. Ong, D. Pines, D. Rainer, R. Singh, J. Thompson, and T. Timusk for useful conversations. I am especially indebted to K. Bedell for numerous suggestions. This work was supported by the U.S. Department of Energy.

¹P. W. Anderson, *Science* **235**, 1196 (1987).

²J. H. Kim, K. Levin, and A. Auerbach, *Phys. Rev. B* **39**, 11633 (1989).

³D. M. Newns, P. C. Pattnaik, M. Rasolt, and D. A. Papaconstantopoulos, *Phys. Rev. B* **38**, 7033 (1988).

⁴N. Nagaosa and P. A. Lee, *Phys. Rev. Lett.* **64**, 2450 (1990).

⁵The t - t' - J model can also be derived from a more complete three-band model; see F. C. Zhang and T. M. Rice, *Phys. Rev. B* **37**, 3759 (1988). This derivation allows $t' \neq J$, a degree of freedom that would allow better fits to experiment but not used in this paper.

⁶S. A. Trugman, *Phys. Rev. B* **37**, 1597 (1988); **41**, 892 (1990); in *Applications of Statistical and Field Theory Methods to Condensed Matter*, Proceedings of the NATO Advanced Study Institute, Evora, Portugal, 1989, edited by D. Baeriswyl, A. R. Bishop, and J. Carmelo (Plenum, New York, 1990).

⁷P. A. Lee, in *High Temperature Superconductivity*, edited by K. S. Bedell *et al.* (Addison-Wesley, Redwood City, CA, 1990).

⁸Y. Tokura, J. B. Torrance, T. C. Huang, and A. I. Nazzari, *Phys. Rev. B* **38**, 7156 (1988).

⁹D. R. Harshman *et al.*, *Phys. Rev. Lett.* **63**, 1187 (1989); A. Weidinger *et al.*, *Phys. Rev. Lett.* **63**, 1188 (1989).

¹⁰P. B. Allen, W. E. Pickett, and H. Krakauer, *Phys. Rev. B* **37**, 7482 (1988).

¹¹M. S. Hybertsen, E. B. Stechel, M. Schlüter, and D. R. Jennison, *Phys. Rev. B* **41**, 11068 (1990).

¹²J. B. Torrance *et al.*, *Phys. Rev. B* **40**, 8872 (1989).

¹³M. Hundley, S.-W. Cheong, Z. Fisk, and J. Thompson (unpublished). Data are for single crystals before oxygen annealing.

¹⁴The spin susceptibility can also be extracted from NMR measurements; see H. Monien, P. Monthoux, and D. Pines (unpublished); M. Takigawa *et al.* (unpublished). At small and moderate doping, the spin susceptibility is close to the measured total susceptibility.

¹⁵H. Takagi *et al.*, *Phys. Rev. B* **40**, 2254 (1989).

¹⁶N. P. Ong, in *Physical Properties of High-Temperature Superconductors II*, edited by D. M. Ginsberg (World Scientific, Singapore, 1990).

¹⁷P. B. Allen, W. E. Pickett, and H. Krakauer, *Phys. Rev. B* **36**, 3926 (1987).

¹⁸N. P. Ong *et al.*, *Phys. Rev. B* **35**, 8807 (1987).

¹⁹Y. Ando *et al.*, *Solid State Commun.* **70**, 303 (1989).

²⁰J. R. Cooper, B. Alavi, L.-W. Zhou, W. P. Beyermann, and G. Grüner, *Phys. Rev. B* **35**, 8794 (1987).

²¹D. C. Johnston, *Phys. Rev. Lett.* **62**, 957 (1989).

²²T. Timusk and D. B. Tanner, in *Physical Properties of High-Temperature Superconductors I*, edited by D. M. Ginsberg (World Scientific, Singapore, 1989).

²³S. Tajima, S. Tanaka, T. Ido, and S. Uchida, in *Proceedings of the Second International Symposium on Superconductivity, Tsukuba, Japan* (Springer-Verlag, Berlin, 1990).

²⁴J. R. Schrieffer, X. G. Wen, and S. C. Zhang, *Phys. Rev. B* **39**, 11663 (1989).